Development of a Variable-Conductance Heat-Pipe for a Sodium-Sulfur (NAS) Battery

*By Kenji Watanabe *, Atsushi Kimura *2, Kenya Kawabata *3, Tomoki Yanagida *2 and Mamoru Yamauchi *2*

ABSTRACT In order to reduce the cost of electric power, efforts have been made to increase utilization efficiency by means of load leveling. One way of accomplishing this is with sodium-sulfur (NAS) batteries, but for these to provide stable long-term service, a temperature control mechanism that operates at high temperatures is required. The variable-conductance heat-pipe (VCHP) described here meets this need. Unlike conventional heat-pipes the VCHP is controllable, and its heat-radiating structure requires no external power source or sensors, and has no moving parts. Installing VCHPs provides a level of heat control ample for the NAS battery, thereby contributing to improved charge/discharge efficiency. This paper describes a VCHP developed for high-temperature applications.

1. INTRODUCTION

In order to reduce the cost of electric power, efforts have been made to increase utilization efficiency by means of load leveling. Sodium-sulfur (NAS) batteries offer an effective way of accomplishing this, storing excess power at night for use during the daytime.

To charge and discharge efficiently, NAS batteries must be kept above 300°C, but if they become too hot due to resistance loss, etc. their lifetime is reduced. Thus to obtain efficient operation over the long term they must be provided with suitable means of controlling temperature. The on-off temperature control available from ordinary heaters, including auxiliary heaters, and heat radiation from the container (casing), however, are inadequate.

The authors therefore set about to provide a heat-radiating mechanism suited to the characteristics of the NAS battery. As a result they have developed this high-temperature variable-conductance heat-pipe (VCHP) for NAS batteries, which provides ample temperature control capability and improved charge/discharge efficiency. This paper provides a description of the VCHP.

2. DESIGNING THE VCHP

Figure 1 shows a conceptual drawing of VCHPs installed on an NAS battery.

* Tokyo Electric Power Co., Ltd.
*2 Power Cable Accessories Div.
*3 Environment and Energy Laboratory

2.1 VCHP Structure and Operation

2.1.1 Comparison with conventional heat-pipe

Figure 2 shows a structural comparison of a conventional heat-pipe and the variable-conductance heat-pipe (VCHP). In the conventional type, a small volume of working fluid is sealed into an evacuated metal container. The working fluid repeatedly vaporizes and condenses as a result of the small temperature difference (or temperature gradient) between the evaporator and condenser sections, and heat is transferred by the latent heat of the working fluid.

The heat-pipe comprises an evaporator section, an adiabatic section and a condenser section, and a wick or mesh is provided in the container to facilitate the circulation of the working fluid. The maximum heat transfer rate, which is the measure of heat-pipe performance, is determined by the wick, the volume of working fluid, and so on, while the working temperature is determined passively by the external heat source, the temperature of the heat radiator (condenser) section, and so on. When the heat-pipe

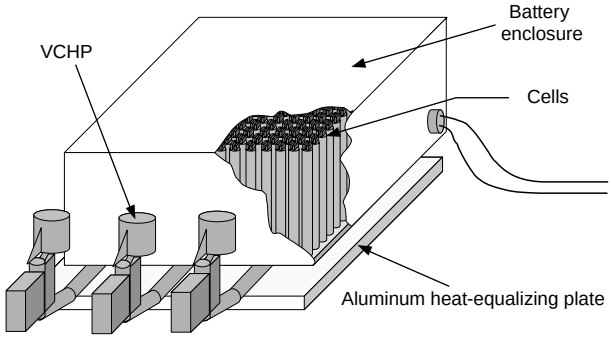

Figure 1 Conceptual drawing of a VCHP installed on an NAS battery

is actually used as the heat-transfer device of an NAS battery, however, it becomes necessary to keep the temperature of the evaporator section constant, or to use on-off operation based on a preset reference temperature.

For these reasons the authors embarked on the development of the VCHP as a heat-transfer device for temperature control of NAS batteries, which, unlike the conventional heat-pipe, is "controllable" and has no need of external power, sensors or moving parts.

Figure 3 compares the heat-radiation characteristics of conventional and variable-conductance heat-pipes. Unlike the conventional heat-pipe, in which the heat radiation rate has a constant gradient relative to temperature, the radiation rate in the VCHP increases rapidly from a given temperature (the radiation onset temperature) until the radiation limit is reached. When the radiation limit is exceeded, it traces a constant gradient, like a conventional heat-pipe. The term "variable conductance" has its origin in this characteristic, and the slope of the line between the radiation onset point and the radiation limit point (hereinafter referred to as the radiation gradient) is an important characteristic of the VCHP.

2.1.2 Operation of the VCHP

Figure 4 is a conceptual diagram illustrating VCHP operation. The VCHP comprises noncondensable gas enclosed in a heat-pipe structure and has a reservoir for the gas. Its operation may be explained in terms of steps (1) and (2) below:

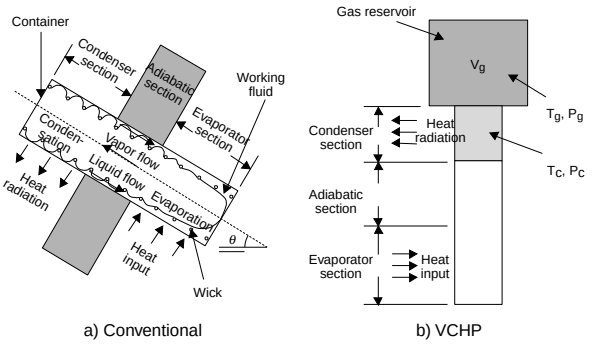

Figure 2 Structural comparison of conventional and variable-conductance heat-pipes

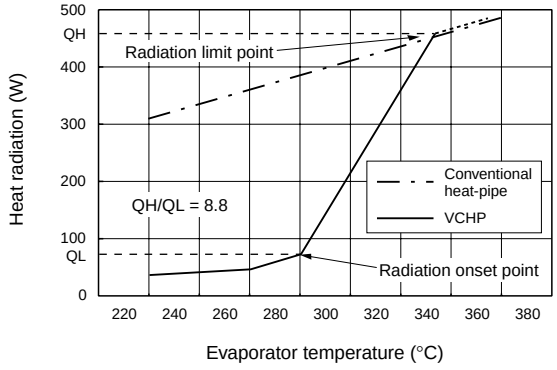

Figure 3 Heat-radiation characteristics of conventional and variable-conductance heat-pipes

(1) The evaporator section is heated by an external heat source and when the working fluid vaporizes the vapor begins to flow toward the condenser section, which is at a lower temperature.
(2) The enclosed noncondensable gas is forced to the end of the condenser (toward the adiabatic section) and reaches equilibrium at saturated vapor pressure for a given working temperature.

The boundary surface (actually a diffusion layer) formed between the working fluid and the noncondensable gas in Step 2 plays an important role in determining the heat radiation rate and the radiation onset temperature. When the boundary surface lies nearer to the condenser section than to the evaporator, the internal heat transfer to the condenser that is characteristic of heat-pipe operation does not occur, and the only radiation is that transferred by the container--a tiny fraction of the maximum heat transfer rate.

In Figure 4 (a), a gradual increase in working temperature is accompanied by a rapid increase in saturated vapor pressure of the working fluid. In contrast there is only a slight increase in the temperature on the noncondensable gas and, since the relationship between pressure and cubic capacity is constant, the boundary surface is pushed out by the working fluid so that the "condenser section that is effective for radiation with admixture of working fluid" migrates toward the gas reservoir. In Figure 4 (b), the region occupied by the working fluid is reduced, and the internal heat transfer rate is still small. If the temperature is further increased, the condenser section that is effective for radiation becomes larger, and the heat radiation rate increases. At the point of maximum heat radiation, the noncondensable gas is totally contained within the gas reservoir. In Figure 4 (c), if the heat radiation rate is greater than the maximum heat input to the evaporator section by the heat source, sufficient heat radiation can be obtained and the temperature of the evaporator section will not increase further.

From the above it can be seen that if the container is filled with a fully adequate volume of working fluid and the optimum volume of noncondensable gas, and is provided with a condenser (radiator) section adequate for heat radiation, the VCHP can deliver appropriate heat radiation

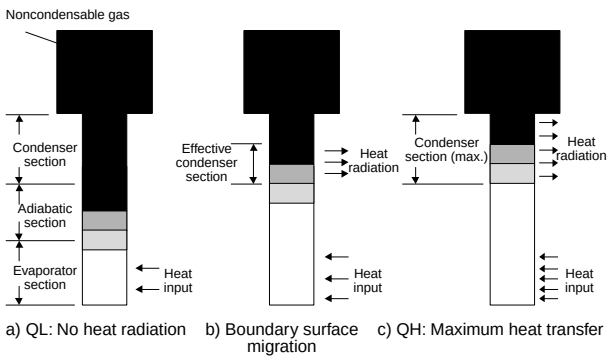

Figure 4 Heat transfer during VCHP operation

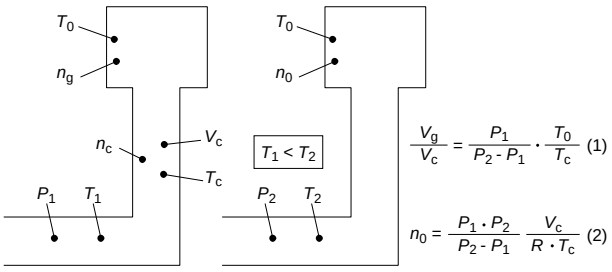

a) QL: Onset of heat radiation b) QH: Maximum heat transfer

Figure 5 Thermal model of a VCHP

between the upper and lower limits of its temperature range.

In considering applications to NAS batteries, if the VCHP is designed so that its lower limit temperature corresponds to the minimum operating temperature (radiation onset point) of the battery and its upper limit temperature to the battery's maximum operating temperature (radiation limit point), it is possible to configure an efficient temperature control mechanism that requires no external power source, sensors or moving parts, and at the same time minimize battery aging.

2.2 VCHP Design

2.2.1 Design model

Figure 5 shows a design model. As described above, the operational sequence involves changes of the volumes and pressures of various substances in a sealed container, and is fundamentally governed by Boyle's law:

$$\frac{V_g}{V_c} = \frac{P_1}{P_2 - P_1} \cdot \frac{T_0}{T_c} \quad (1)$$

$$n_0 = \frac{P_1 \cdot P_2}{P_2 - P_1} \cdot \frac{V_c}{R \cdot T_c} \quad (2)$$

where:

V_g is the volume of the gas reservoir,
V_c is the volume of the condenser section
P_1 is the radiation onset pressure (evaporator section)
P_2 is the maximum radiation pressure (evaporator section)
T_1 is the radiation onset temperature (evaporator section)
T_2 is the maximum radiation temperature (evaporator section)
T_c is the gas temperature in the condenser section
T_0 is the temperature of the gas reservoir
n_g is the number of moles of vaporized working fluid
n_c is the number of moles of gas in the condenser section
n_0 is the number of moles of mixed gas

It is then possible, by substituting into the above equation design conditions--T_1 or T_2, V_c, P_1 or P_2 and so on, to establish the volume of the gas reservoir, volume of working fluid, and initial gas charge. Specifically the ratio of volumes V_g/V_c contributes to the temperature control properties, which improve as V_g becomes greater than V_c.

Table 1 shows the specifications of the VCHP.

Table 1 VCHP Specifications

Item	Specification	
Saturated (max.) heat transfer rate	1000 W (at maximum temperatures shown below)	
Temperature control	Average evaporator temperature	285 +3°C -1°C
	Temperature range	Temperature rise Δt = not more than 28°C
	Other	Dryout does not occur
Structure	Length of evaporator section	approx. 1400 mm
	Height of main unit	approx. 900 mm
	Other	Battery contact by means of heat-equalizing plate

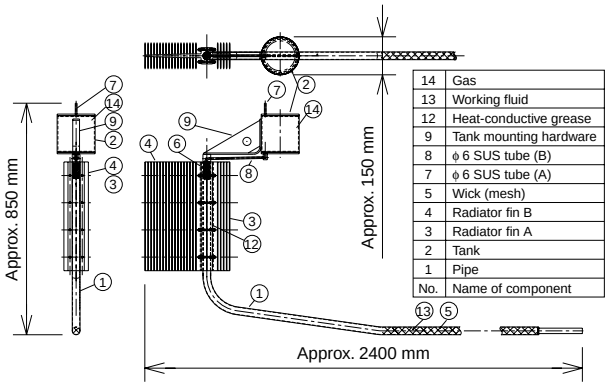

Figure 6 Schematic of a VCHP

2.2.2 Materials and structure

Figure 6 is a schematic of a VCHP.

(1) Working fluid

The main differences between a VCHP and a conventional heat-pipe are that its working temperature and the maximum temperature at saturation exceed 300°C. VCHP operation under such conditions owes much to the operating temperature range of the work-

ing fluid. Accordingly it was decided to use as working fluid a mixture of diphenyl and diphenyl ether, equivalent to DOWTHERM A.

(2) Noncondensable gas
Although nitrogen, helium and xenon were all possible candidates for use as the noncondensable gas, it was decided, for reasons of safety, low thermal conductivity and cost, to use argon. The volume of the gas charge was determined from the model, and the gas pressure was monitored.

(3) Container
If the combination of working fluid and container is not appropriate, reactive gas may be generated within the container degrading control properties and leading eventually to a drop in the maximum heat transfer rate. It is also impossible, due to the temperature range employed, to use the copper that is used for conventional heat-pipes, and it was decided, for environmental and other reasons, to use stainless steel.

The model was also used to determine the volume of the gas reservoir and the diameter of the pipe, and the overall configuration of the VCHP. The container was designed as a pressure vessel and pressure-resistance calculations were used to determine wall thickness.

The structure also inhibits the entry of working fluid into the reservoir due to bumping, and, in the event that entry should occur, capillary tubes are provided linking the gas reservoir and the condenser section, to allow recirculation. Figure 7 shows the mechanism for preventing working fluid backflow.

(4) Wicks
The design provides for a basically gravity-driven method of working fluid circulation, but to facilitate return to the condenser section after heat radiation and to compensate for the greater distance of the evaporator section, a wick is provided to equalize heat and guard against excess localized heat input.

(5) Radiator fins
To allow for the required heat radiation rate and air cooling by natural convection, and because of the temperature difference between absorption and radiation of heat, a compact fin configuration was adopted, providing a suitable heat-dissipating area. The fins are attached to the VCHP by bolts.

(6) Parts interfaces
Heat-conductive compound was used at the interfaces between the fins and the VCHP, and between the VCHP and the heat-equalizing plate. It would have been possible to use welded connections at the interfaces but this method was preferred from the standpoint of facilitating removal and replacement during transportation and inspection. Since the prime constituent of the compound was oil, there was a problem in terms of maintaining thermal conductivity, plasticity and adhesion at high temperatures, but it was possible to obtain a compound that satisfied performance requirements.

3. VERIFICATION OF VCHP PERFORMANCE

3.1 Testing Equipment

Figure 8 is a block diagram of the testing equipment, simulating the VCHP attached to the battery unit in a design that takes account of heat radiation to the outside of the device. The input of heat to the VCHP was set so as to obtain a maximum heat transfer rate of 1000 W. Heat measurement was carried out at several points on the evaporator, adiabatic and condenser sections, and pressure measurements were carried out on the gas reservoir.

3.2 Test Results

3.2.1 Temperatures and gradients

Figure 9 shows temperature distribution in VCHPs under test. At a heat input of 90 W, achieving the radiation onset temperature of 285°C, the condenser (heat radiator) section was at about 20°C, or around ambient temperature. As heat input increased, condenser temperature rose, and at a heat radiation rate of 1000 W, temperatures reached about 120°C at the top end of the condenser and about 90°C at the bottom end. From this it can be seen that the

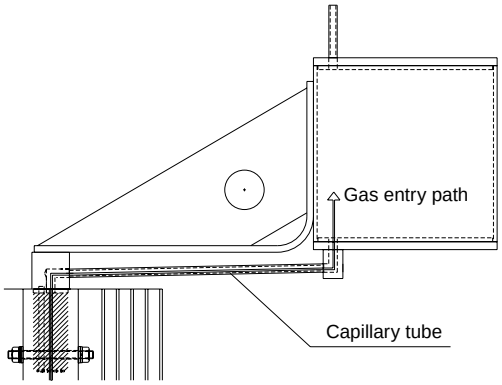

Figure 7 Mechanism to prevent working fluid backflow

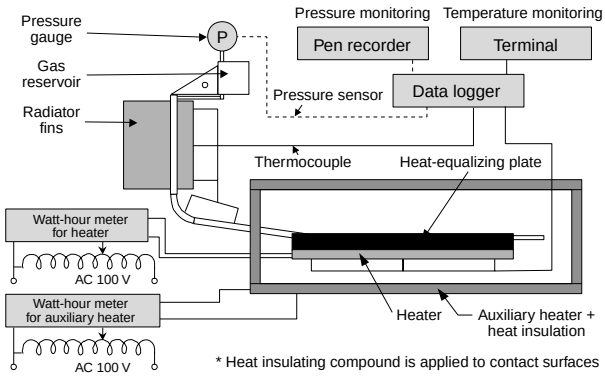

Figure 8 Block diagram of testing equipment

VCHP was operating normally. There was also an increase in the temperature gradient as heat input increased, but this shows that condenser temperature rose gradually from the evaporator side, and demonstrates the stability of its characteristics.

3.2.2 Heat radiation characteristics

Figure 10 shows the heat radiation characteristics found when heat input and heat radiation were in equilibrium. This test was conducted on three samples for verification purposes, and all three came within specification for radiation onset temperature. The radiation gradient was also high, with all three samples exhibiting a temperature control range Δt of not more than 10°C at saturation (maximum) heat transfer rate, an excellent result that satisfied specifications. From this we may conclude that control performance and heat radiation characteristics are stable and uniform across product samples.

3.2.3 Relationship between working fluid volume and gas charge volume

The following tests were performed to verify the difference in characteristics due to errors in the volume of gas charged.

(1) Changes in volume of working fluid

Figure 11 shows changes in the heat radiation characteristics when the volume of the working fluid was changed plus or minus 10% with respect to the standard volume, maintaining constant gas charging pressure. When working fluid volume was low there was no problem with the radiation gradient, but there was a rise in the radiation onset temperature. When there was an excess of working fluid, on the other hand, there was no problem with respect to radiation onset temperature, but as the rate of radiation increased there was a tendency for evaporator temperature to rise. This is due to the fact that the volume of gas charged varied with increases and decreases in the volume of working fluid, since the charging pressure of the gas was constant. In practice charging error is in the neighborhood of 1%, and there is no change in control characteristics due to error in the volume of working fluid charged.

(2) Volume of gas charge

Figure 12 shows changes in the heat radiation characteristics when the volume of the gas charge was changed plus or minus 2.5% with respect to the standard volume, maintaining constant working fluid volume. When the gas charge volume was large the radiation onset temperature rose. As was explained in Section 2 above, the increase in gas pressure had the effect of pushing the boundary surface toward the condenser. In practice charging error is in the neighborhood of 0.1%, and there is no change in control characteristics due to error in the volume of gas charged.

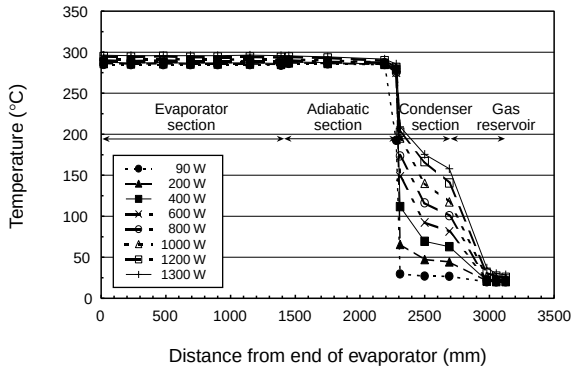

Figure 9 Temperature distribution in VCHPs under test

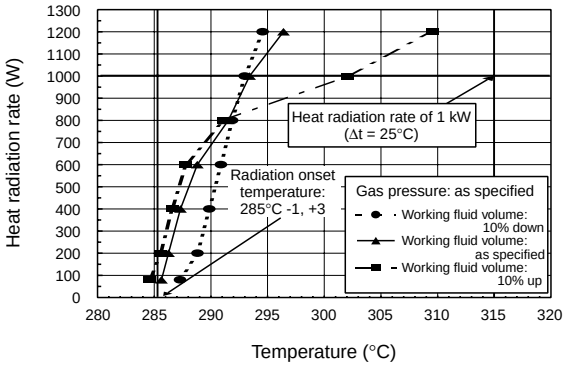

Figure 11 Influence of working fluid volume on heat radiation characteristics

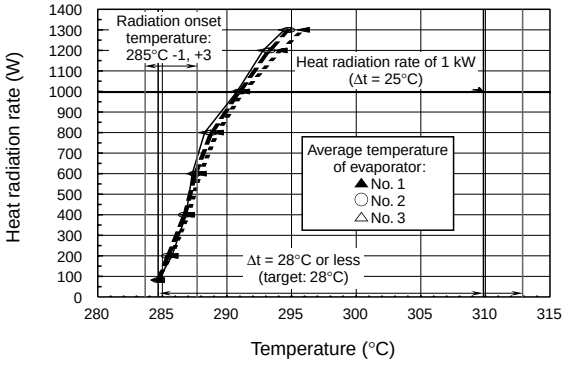

Figure 10 Heat radiation characteristics

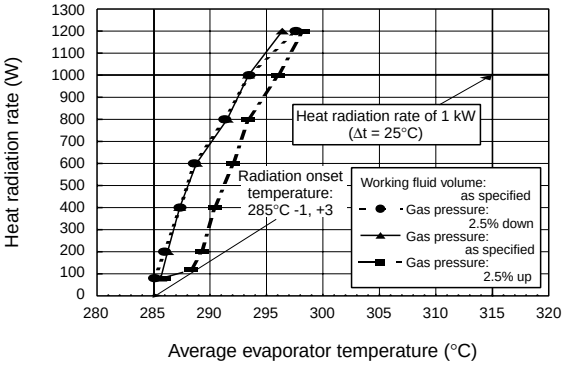

Figure 12 Influence of gas charging pressure on heat radiation characteristics

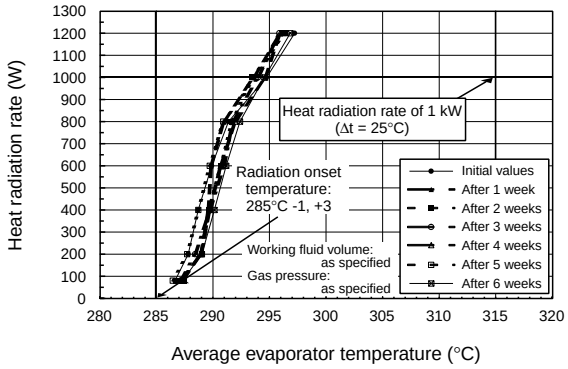

Figure 13 Results of life tests

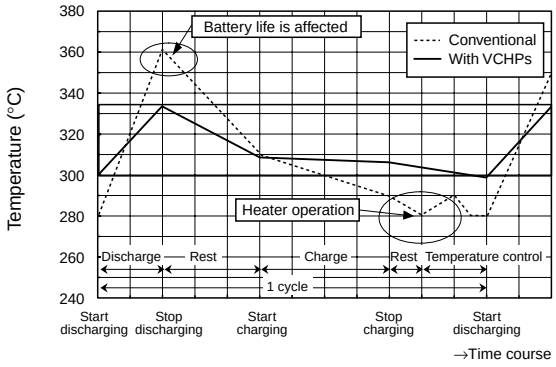

Figure 14 Comparison of time courses of NAS battery temperature with and without VCHPs

3.2.4 Long-term reliability

Figure 13 shows the results of life tests, which involved operating the apparatus for six weeks. Based on actual battery operation, a duty cycle of five days on and two days off was adopted. The radiation gradient was constant, and long-term reliability was obtained. Variations in characteristics are thought to be a matter of variations in temperature measurement; the characteristics themselves do not change significantly. Life tests of actual apparatus were carried out for from three months to as long as one year.

4. EFFECT WITH NAS BATTERIES

The following material makes clear the advantages of using VCHPs with NAS batteries. Figure 14 shows the changes in the time course of NAS battery temperature due to the use of VCHPs.

4.1 Temperature Control Characteristics

Temperatures were controlled within a narrower range than was specified in the design values. Results of measurements at various points demonstrated that the temperature of the evaporator section exhibited outstanding uniformity in the length direction.

4.2 Reaction to heat input

Radiation characteristics (when heat input is increased, raising the temperature of the evaporator section) form the basis for determining whether VCHPs can be applied to temperature control for NAS batteries. As noted in Section 3, the VCHP is superior in that its radiation onset temperature is determined by the design, so that at temperatures below this value it has a low heat transfer rate attributable to the container itself but above the onset temperature the radiation rate rises abruptly and does not diminish even in the high-temperature range.

4.3 Battery Life and Efficiency

NAS batteries provided with VCHPs were maintained within the limiting temperatures for aging even when operated continuously at the initial radiation rate. And the target level of efficiency was achieved even when operating at the terminal period of its service life (when the radiation rate was increased above the rated value).

5. CONCLUSION

As a result of efforts to provide a radiation mechanism to control the temperature of NAS batteries, the authors have developed a VCHP for high-temperature applications which has ample temperature control capability resulting in improved charge/discharge efficiency. Work is going forward to further reduce the cost of the apparatus, and to extend applications to other controllable heat radiation mechanisms.

Manuscript received on May 22, 2000.